

Dynamics and Performance of Susceptibility Propagation on Synthetic Data

Erik Aurell^{1,2,3}, Charles Ollion^{1,3}, and Yasser Roudi⁴

¹ ACCESS Linnaeus Center KTH-Royal Institute of Technology, 100 44 Stockholm, Sweden

² Department of Informatics and Computer Science, Aalto University, Finland

³ Department of Computational Biology, AlbaNova University Centre, 106 91 Stockholm, Sweden

⁴ NORDITA, Roslagstullsbacken 23, 10691 Stockholm, Sweden

the date of receipt and acceptance should be inserted later

Abstract. We study the performance and convergence properties of the Susceptibility Propagation (SusP) algorithm for solving the Inverse Ising problem. We first study how the temperature parameter (T) in a Sherrington-Kirkpatrick model generating the data influences the performance and convergence of the algorithm. We find that at the high temperature regime ($T > 4$), the algorithm performs well and its quality is only limited by the quality of the supplied data. In the low temperature regime ($T < 4$), we find that the algorithm typically does not converge, yielding diverging values for the couplings. However, we show that by stopping the algorithm at the right time before divergence becomes serious, good reconstruction can be achieved down to $T \approx 2$. We then show that dense connectivity, loopiness of the connectivity, and high absolute magnetization all have deteriorating effects on the performance of the algorithm. When absolute magnetization is high, we show that other methods can work better than SusP. Finally, we show that for neural data with high absolute magnetization, SusP performs less well than TAP inversion.

PACS. 75.10.Nr, 02.50.Tt, 05.10.-a

1 Introduction

Problems in Statistical Mechanics and those in Statistical Inference can be thought of as being the inverses of each other. In statistical mechanics one is usually given a Gibbs distribution and is asked to compute moments of some observables. In statistical inference, one is given a set of observables and is asked to reconstruct the distribution that generated them. Although the two fields have traditionally been developed separately, recently the connections and similarities have been highlighted, see *e.g.* [6].

A paradigmatic scenario in this direction is the Inverse Ising problem, that is finding the couplings of an Ising model given data *e.g.* mean magnetizations and pairwise correlations. Two strands of questions in biology have recently motivated this problem. The first one comes from Neuroscience. While traditionally it has only been possible to record simultaneously from a few neurons at a time, for special cases, *e.g.* retinal cells recordings from hundreds of neurons are now possible, and techniques allowing for many more are on the horizon. The problem is then to infer functional connectivities between neurons from these recorded multi-neuronal spike trains. [14, 2, 13, 11]. Second, global gene expression measurements by *e.g.* microarray technologies have been around for more than a decade, and a standard way to analyse them is through co-

expression, *i.e.* correlation of expression of genes or groups of genes across different conditions. Correlation is not causation. If, in fact, the gene expression measurements are snap-shots of a probability distribution generated by an Ising model, then the most significantly coupled genes will be the ones most strongly coupled in the Ising model, not the most strongly correlated, and this is then another way to classify genes as similarly or not similarly expressed [4].

The inverse Ising problem is a difficult combinatorial optimization problem in the class known as “NP-hard”. In theory, only approximate schemes, or methods that take more than polynomial time to find the answer are possible. Boltzmann Learning [1] is an iterative method where in one step the correlation functions are computed given an Ising model, and in another step the Ising model couplings are modified to adjust to data. In principle, Boltzmann learning can be employed to find the couplings with arbitrary accuracy given accurate data and sufficient time, but the slow convergence of the Boltzmann learning makes it a very inefficient algorithm for most practical purposes. The main approximate schemes using means and correlations are inversion of the correlation matrix (“naive mean-field theory”) as used in [4], Thouless-Anderson-Palmer (TAP) formula [3, 18], Independent Pairs Approximation [13] and the perturbative scheme of an auxiliary statistical mechanics model of Sessak and Monasson [15]. If the sample data

can be used as such (and not only via means and pairwise correlations), a linear regression can be performed on a link-by-link basis, which is quite powerful when the underlying matrix of couplings is sparse [10].

In this paper, we study the recently introduced Susceptibility Propagation (SusP), an approximate scheme also based on means and correlations [7]. SusP is a message-passing algorithm which is derived by using the Fluctuation-Response theorem to the update rules of Belief Propagation. Although there are particular features specifically for Ising spins, on one level, and more generally, SusP can be considered as Boltzmann Learning scheme, where the correlation functions are computed by Belief Propagation instead of (much more slowly) by Monte Carlo. Belief Propagation is based on messages exchanged between each pair of nodes [20]. SusP uses such messages as well as the derivatives of these messages with respect to the field at a third node, yielding in the end messages involving triplets of nodes. SusP is fairly sensitive to the accuracy by which the correlation functions are known [5, 9].

Our contributions in this paper are as follows. In the paradigmatic Sherrington-Kirkpatrick model, also studied in [7] and [5], we provide numerical evidence for a phase transition between *reconstructible* and *non-reconstructible* phase, relative to the SusP algorithm. Perhaps surprisingly, this transition is not at the spin glass transition ($T_c = 1$) but some distance into the disordered paramagnetic phase ($T_{SusP} \approx 4$). We show that in the non-reconstructible but still disordered phase, SusP almost converges, in the sense that trajectories of the updates according to SusP come close to a marginally unstable fixed point, and spend a long time in the neighborhood of that fixed point before eventually diverging. We introduce a heuristic stopping criterium for SusP in this region, and with a reasonable criterion for quantitative reconstruction we are able to push the threshold for (approximate) reconstruction down to $T_{SusP} \approx 2$. We also investigate how the performance of SusP on a Sherrington-Kirkpatrick model depends on external field (magnetization). Going beyond the Sherrington-Kirkpatrick model, we considered various sparse models, where many (or most) of the potential couplings are zero. In particular, we show that SusP works very well on a randomly diluted Sherrington-Kirkpatrick model, and in this scenario clearly outperforms other approximate schemes. Furthermore, we show that, given a fixed sparsity, the reconstruction is better on a randomly connected graph compared to a regular lattice. Finally, we show that for *in silico* neural data for which TAP inversion and Sessak-Monasson approximations work well [13, 11], SusP appears to be out-performed by these two simpler schemes.

2 General Setting

Susceptibility propagation is a fairly complicated algorithm, which, for completeness, we describe in Appendix. To be able to refer to a definite formula, let us however state that one central step in SusP is the inversion

$$J_{ij} = \tanh^{-1} \left(\frac{C_{ij} - \tanh h_{i \rightarrow j} \tanh h_{j \rightarrow i}}{1 - C_{ij} \tanh h_{i \rightarrow j} \tanh h_{j \rightarrow i}} \right) \quad (1)$$

where $h_{i \rightarrow j}$ and $h_{j \rightarrow i}$ are Belief Propagation messages and C_{ij} are auxiliary quantities encoding gradients of messages, the observed correlation between spins i and j , as well as the observed magnetizations of spin i and spin j . After an update of the J_{ij} the messages and their gradients are updated according to equations given in Appendix, where the J_{ij} enter parametrically, and this procedure is repeated until convergence. When this procedure converges, and how accurate it is when it does are important points to understand here. In this Section we describe how we address these two points in this paper.

The overall idea is to compute mean magnetizations and pairwise correlations from a *known* Ising model and use them to reconstruct the model back. We can then illustrate reconstruction by a scatter-plot of the inferred couplings J_{ij}^{SusP} versus the (known) true couplings J_{ij} . A straight line scatter plot of slope one indicates a successful reconstruction. This can be quantified by the correlation coefficient of the scatter plot (R), and the P-value of a the null hypothesis that the reconstructed couplings are equal to the true ones. Alternatively, we can quantify the quality of reconstruction in one of our test cases by the Δ -measure of [7, 5]:

$$\Delta = \frac{1}{\text{std}(J_{ij})} \sqrt{\frac{2}{N(N-1)} \sum_{i < j} [J_{ij}^{SusP} - J_{ij}]^2} \quad (2)$$

The first test case is the Sherrington-Kirkpatrick model [16] of N spins, $\boldsymbol{\sigma} = (\sigma_1, \dots, \sigma_N)$ and Boltzmann distribution

$$\Pr(\boldsymbol{\sigma}) = \frac{1}{Z} \exp \left[\beta \sum_i h_i \sigma_i + \beta \sum_{i < j} J_{ij} \sigma_i \sigma_j \right], \quad (3)$$

in which $\beta = 1/T$ is the inverse temperature and the couplings J_{ij} are drawn from a zero mean Gaussian distribution with variance $1/N$. This case has already been considered by [7], where it was shown that SusP outperforms several other reconstruction methods in the high temperature and zero external field regime (small β , all h_i zero), and also by [5] where it was shown that SusP is sensitive to noise in the correlation functions. Our contribution, for this family of test cases, is a precise determination of the threshold in the low temperature regime where SusP ceases to converge (in Section 3), and an extension of the analysis to the case with non-zero external fields (in Section 4). We further introduce a modification of the SusP stopping criterion pushing the boundary of (approximate) reconstruction to lower temperatures.

Motivated by the ‘‘folklore theorem’’ that message passing techniques work best on locally tree-like graphs, we also study the effect of network geometry on the convergence of SusP. The underlying graph of the SK model is fully connected with many loops, so this is presumably a

rather difficult case for SusP. We therefore consider randomly diluted SK models, where a fraction $(1 - c)$ of the couplings to each node are set to 0 while cN randomly picked couplings are drawn from a Gaussian distribution with variance $1/(cN)$ or $1/N$. In the same spirit, but in the opposite direction, we also consider SusP on a lattice graph, where each spin is connected to its cN nearest neighbors.

Finally, we apply SusP to infer functional couplings in data generated from a simulated neural networks. Using inverse models to describe the statistics of neural data has been one of the very active fields of research lately [14, 17, 12, 2] and various approximations from statistical mechanics have been studied for the inference of Ising model applied to neural data [13], showing that TAP inversion and Sessak-Monasson approximations work very well for this type of data. Here we show that for fine time bins (10ms), SusP is outperformed by these simpler approximations.

To end this Section: for small samples, *i.e.* $N \leq 20$, we can calculate the means, $m_i = N^{-1} \sum_{\sigma} \Pr(\sigma) \sigma_i$, and correlations $C_{ij} = N^{-1} \sum_{\sigma} \Pr(\sigma) \sigma_i \sigma_j - m_i m_j$ by exact enumeration and summing over all the 2^N states. For larger values of N , we use Monte Carlo sampling to estimate the means and correlations since the exact summation is not feasible. For larger values of N the means and correlations are therefore always more or less noisy.

3 Convergence at Low T

In this Section we study convergence of the SusP algorithm on the test case of an SK model at zero external field. Temperature, as in Eq. (2), should be understood as a shorthand of the overall size of the couplings. It is well-known that this model has a phase transition to a spin glass phase at $T_c = 1$. When the temperature is high, the SusP algorithm can find the couplings very accurately, with a reconstruction error that is essentially limited by the quality of the measured means and correlation and the machine accuracy. We do not show these data, already obtained by [5], but only point out that in the high temperature regime other reconstruction methods also work, and importantly the high temperature TAP inversion technique would work well [3, 18]. Therefore, SusP can only be a competitive reconstruction method at high temperature if both the quality criteria are very strict, and also the means and correlations are known very accurately.

The interesting case is, therefore, at low temperatures, where most reconstruction techniques have difficulties, and where the SK model approaches the spin-glass phase. One way in which the procedure sketched above and embodied by Eq. (1) can definitely fail to converge is if the argument of the right hand side of Eq. (1) eventually becomes larger than one in absolute value. If so, inversion is not possible (imaginary J_{ij}). A convenient empirical tool to monitor algorithm convergence and performance on families of large instances is a *pivoting plot*. A number of random instances are generated and the convergence or performance of the

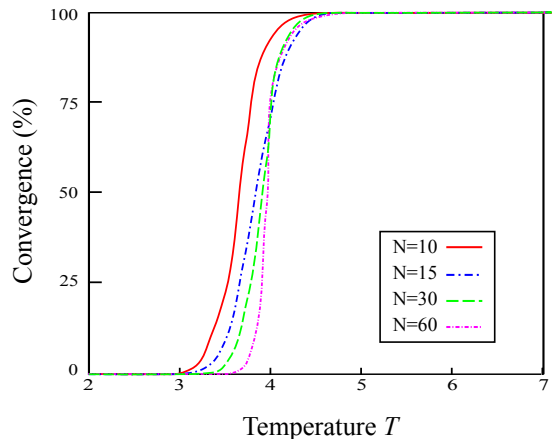


Fig. 1. Convergence of SusP with no stopping criterion or damping factor. A phase transition seems to occur around $T_{SusP} \approx 4$. We can conjecture that at higher N the phase transition will be sharper.

algorithm is determined across the family. The fraction of good outcomes then varies with the size of the instances and a parameter describing the family. In the case at hand, this parameter is the temperature T , and the size is N . In favorable cases the location of the transition between high and low fractions of good outcomes depend only weakly on N and becomes sharper as N grows, giving rise to a characteristic “pivoting” shape of the cumulative empirical probability distributions.

As shown in Fig. 1, for SusP on the SK model, there is clear pivoting and a threshold separating a convergent from a non-convergent phase. This transition occurs at $T_{SusP} \approx 4$. To avoid this convergence problem, the update rule can be modified with a damping factor [5]. There are two problems, however, with the low-T convergence even when the damping factor is used. First, the damping factor makes the convergence slow for low T because strong damping ϵ must be employed. Second, we have also observed that for sufficiently low T , although the imaginary J problem can be avoided by using the damping factor, the algorithm fails to converge even with very small ϵ .

The behavior of the algorithm on representative instances are exemplified in Fig. 2, where we show total reconstruction error as well as the dynamics of one example coupling versus the number of iterations used in the algorithm. It is clearly seen that even for small T , where the algorithm will eventually diverge, there is a plateau where the couplings remain almost constant for many iterations. In fact, comparing with the dynamics of J at larger T , where convergence does occur, we see that the dynamics is then qualitatively similar, only the plateau then being also the asymptotically steady state. In other words, the dynamics of the SusP algorithm close to the solution has a direction which changes from marginally stable to marginally unstable as T decreases, and this can be seen to be the cause of bad reconstruction in this regime. Consequently, by stopping the algorithm when changes in J

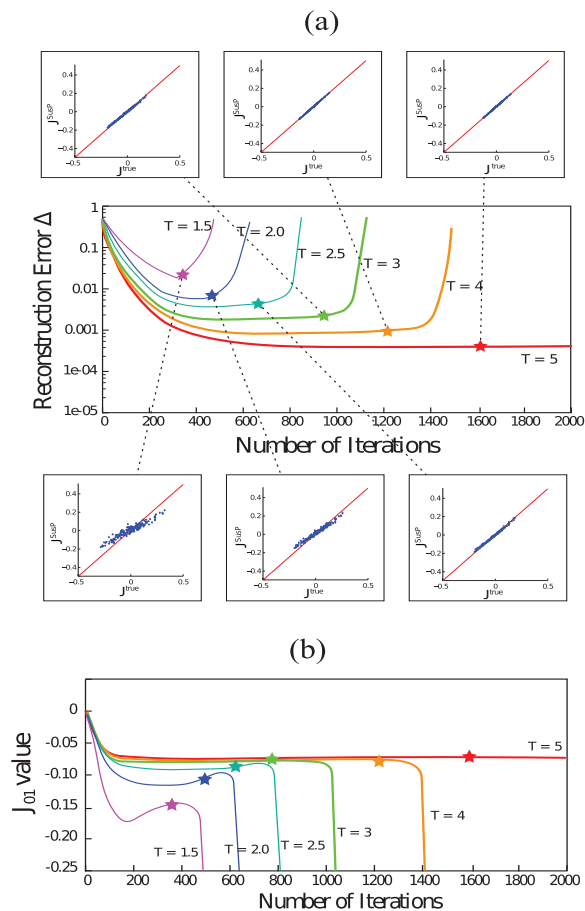


Fig. 2. The reconstruction error as the algorithm proceeds (a), and the dynamics of one particular coupling J_{01} (b) as the algorithm proceeds, and for different temperatures. The stars show where the stopping criterion Eq. (4) is satisfied and the associated scatter plots show the inferred couplings versus those of the original model.

from one iteration to the next are small, long before the argument of the right hand side of Eq. (1) turns negative, we can hope to achieve good reconstruction also at very low temperatures.

This is indeed possible, as shown in the scatter plots in Fig. 2 where we have shown the inferred couplings versus true couplings after t iterations where

$$|J_{ij}^t - J_{ij}^{t-1}| > |J_{ij}^{t-1} - J_{ij}^{t-2}| \quad (4)$$

for at least 90% of the pairs of i and j . Fig. 3, shows how according to the criterion of at most 5% reconstruction error (measured by Δ) reconstruction is possible at lower temperatures, down to new threshold T_{SusP} approximately equal to 2.

4 Influence of varying the external field and mean magnetization

The results shown in the previous section as well as those reported in [5] were all run on data from a model with-

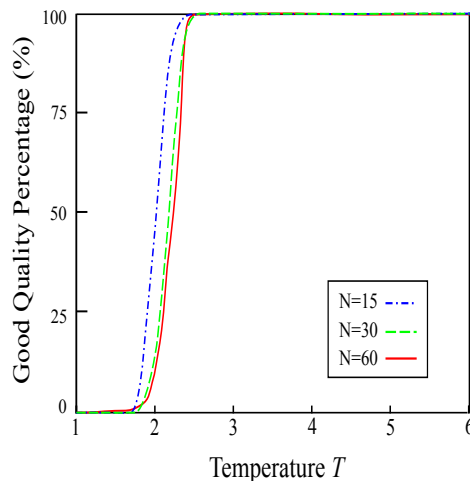


Fig. 3. Percentage of good reconstruction with stopping criterion. A reconstruction is considered good when the error Δ is below 0.05. There is a rather sharp threshold at temperature close to 2.

out external field, *i.e.* when $h_i = 0$ for all i . In this case, because of the symmetry of the problem the mean magnetizations are all zero (if calculated exactly), and fluctuate around zero when computed by Monte Carlo sampling. This raises the question of the effect of magnetization and external fields on the reconstruction error.

As described in Appendix, SusP first computes the couplings in a loop of alternate steps of changing J_{ij} and Belief Propagation updates; the external fields h_i are only computed in a Belief Propagation output step. Similarly to other schemes such as TAP, reconstruction of the external fields can therefore essentially never be better than the reconstruction of the couplings. The questions are therefore, first, how well the couplings are reconstructed if the magnetizations are sensibly different from zero, and second, if reconstruction quality is degraded in the final step from the couplings to the external fields. This is an important issue to investigate since in many real life applications, *e.g.* neural data binned at small time bins, one would be dealing with highly magnetized variables.

On the first point, in Fig. 4, we show that reconstruction of the couplings by SusP is degraded, either as a function of external fields, or as function of mean magnetization. Here we have used a uniform external field applied to all spins. As a function of external fields the loss of reconstruction quality is smooth, while as a function of magnetization it is abrupt, and concentrated in a narrow range close to $|m| \approx 1$, essentially due to the fact that as $|m| \rightarrow 1$ one has $h = \tanh^{-1}(m)$ [12]. The dependence is sharper at higher temperature, *i.e.* when SusP in zero magnetization works well.

On the second point, we do not observe significant degradation going from the couplings to the external fields. As shown in Fig. 5, the quality of this reconstruction also degrades at lower temperatures, as is the case for the couplings.

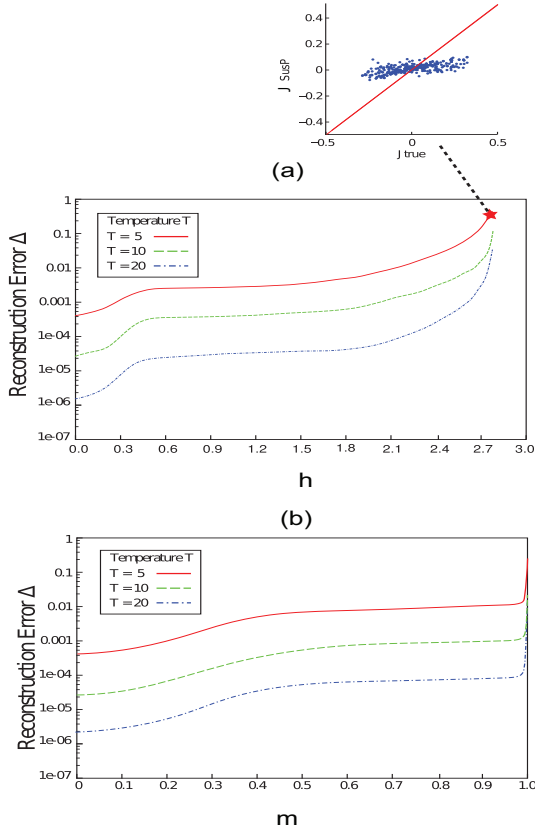


Fig. 4. Reconstruction error as a function of external field (a) and mean magnetization (b). At all temperatures and network sizes tested, increasing the absolute magnitude of the magnetization by increasing the external field has a negative effect on the reconstruction.

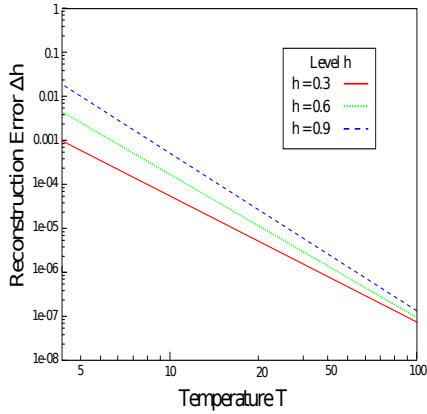


Fig. 5. The reconstruction error Δh (mean value of the absolute error of each field) as a function of the temperature T .

5 Geometry and sparsity of the graph

SusP has its root in the Belief Propagation algorithm. It is well-known that the BP is exact on trees, *i.e.* graphs without loops [20]. We would then expect that the performance of SusP is also influenced by the presence or absence of loops in the model that generated the data.

To test this hypothesis, we first studied how the sparsity of the connectivity pattern of the model influences the reconstruction. We thus generated data from a SK model in which a fraction c of the couplings are put to zero while the rest are drawn either from a Gaussian distribution with variance $1/N$, or with $1/(cN)$. The results are shown in Fig. 6 where we plot the reconstruction error versus the sparsity c . We can observe a decrease in the reconstruction error as c decreases, thus concluding that SusP works better when the connectivity is sparse. For almost all values of c , the positive effect of a sparser graph on the reconstruction error is suppressed when one has stronger connections, *i.e.* when the variance of the couplings are taken to be $1/(cN)$.

To understand how the graph geometry influences SusP, we altered the geometry of connections, at fixed c , from a random connectivity to a 2D rectangular lattice with each node being connected to cN other closest nodes to it. This way, at a fixed sparsity, we essentially increase the loopiness of the graph, by inducing local small loops. As shown in Fig. 6 the presence of these local loops increases the reconstruction error. For a given connectivity, a random sparse graph has fewer local loops than the lattice one, which explains why the reconstruction is better on random sparse than on a lattice.

6 Tests on Neural Data

The Ising model has been used in a number of studies for modeling the statistics of multi-neuron spiking patterns of binned spike trains. They were shown to provide a good model for spike patterns over N neurons, if the average number of spikes generated by all N neurons in a time bin is small [14, 12]. Various approximations have been studied in [13, 11] where TAP inversion and SM approximations were shown to provide good estimates of the functional couplings. In what follows we study the performance of SusP on synthetic neural data generated from a simulated cortical network model and compare them with TAP. For details of the simulations see [13].

Fig. 7 shows the results of TAP, and SusP as compared to the results of Boltzmann learning for neural populations of size $N = 40$ and $N = 100$. This figure shows that for this type of data TAP outperforms SusP, particularly for large N . One reason for this could be the fact that to make a binary representation of the spike trains, one has to bin them to small time bins, typically of size $\delta t = 10\text{ms}$. This yields a mean probability of spike per bin of ~ 0.9 or mean magnetization of ~ -0.7 . Our previous analysis in section 4 did provide the conclusion that large absolute magnetization has a negative effect on the performance of SusP.

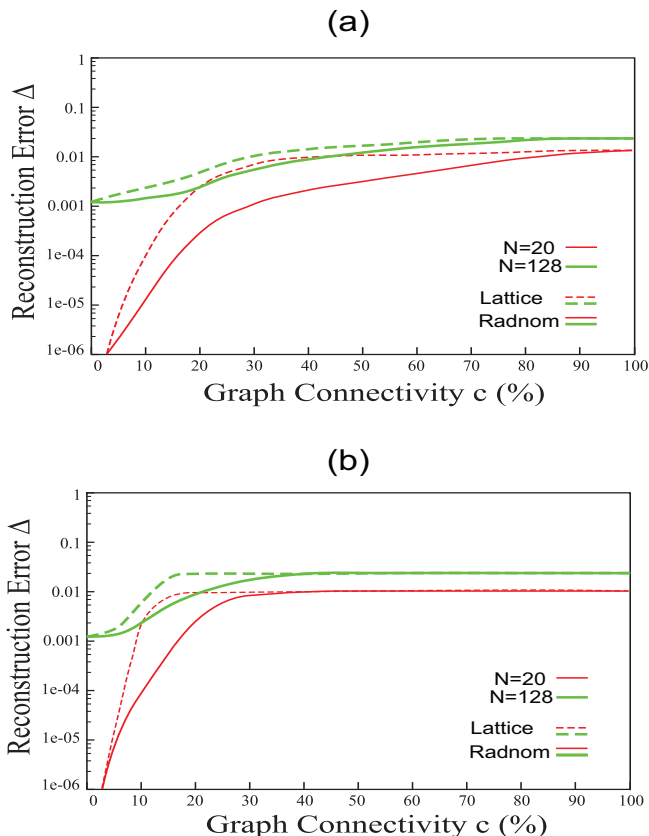


Fig. 6. The influence of the sparsity and connectivity pattern on SusP. (left) The reconstruction error is shown versus the fraction of connections for different sizes both in the case of a random graph and a 2D lattice. In this case the variance of the couplings scale as $1/N$ independent of c . (right) This is the same as a, except that the variance of the couplings now scale as $1/cN$. SusP appears to work better on sparser and less loopy graph.

7 Discussion

The ability of experimentalists to observe the activity of a large number of elements in biological networks needs to be accompanied by mathematical tools to analyse the high dimensional recorded data. One approach for doing this it to develop analytical and numerical tools to infer a probability distribution with a small number of parameters from the recorded data, small compared to the possible number of states of the system. The fitted model can then be used to generate synthetic data, or it could be used to learn something about the network that generated the data, *i.e.* to learn functional connections between the elements.

The Ising model is probably too simple a model for many real life purposes and the inferred couplings may not correspond to real physical interactions, depending on the real underlying physical system [13]. However, it provides an excellent platform to study the analytical and theoretical aspects of the problem. Many of the hurdles encountered in the inverse Ising problem are likely to be present when dealing with more complicated models. De-

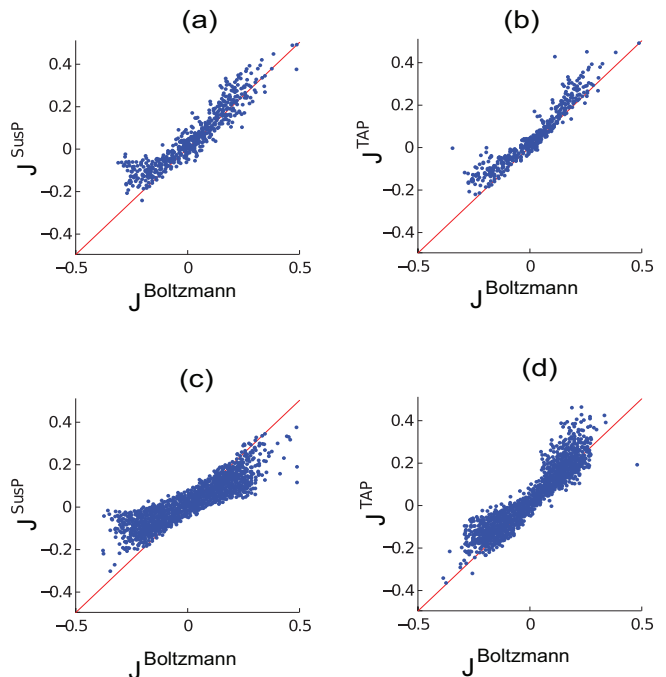


Fig. 7. Comparing SusP (left) and TAP results (right) versus the Boltzmann learning for $N = 40$ (up) and $N = 100$ (down) for synthetic neural data binned at $\delta t = 10$ ms.

veloping and analyzing approximate and iterative methods for inverse Ising problems has therefore attracted a lot of attention in the past few years.

The SusP algorithm is the result of the last effort in this direction. Not surprisingly, it exhibits complex dynamical behaviors when applied to loopy graphs some of which we studied here. Importantly, the simplest implementation of the algorithm exhibits a dynamic phase transition to a non-convergent regime at $T_{SusP} \approx 4$, *i.e.* higher than the equilibrium phase transition of the SK model. Our numerical experiments show that for a range of temperatures below T_{SusP} the lack of convergence of the algorithm is due to the presence of an unstable direction in the trajectory of the couplings, such that the algorithm gets close to the true couplings, stays there for a while and then moves away from it. Exploiting this fact, it is possible to perform good reconstructions down to $T_{SusP'} \approx 2$. Whether it is possible to avoid such a direction all together requires a more detailed study of the dynamics of the couplings during the learning process. It would also be interesting to see whether loop correction methods such as those developed for Belief Propagation [8] could be also employed in SusP.

Two new observations of the SusP algorithm have been made in this paper. One positive, albeit expected, is that SusP works much better (at large typical couplings) on sparse graphs. If it is known a priori that the underlying graph is sparse, then SusP should be very competitive to other schemes using means and correlations such as TAP or Sessak-Monasson. However, this is also the regime where the recent l_1 reconstruction of Ravikumar, Wainwright and Lafferty [10] provably works. More experimen-

tation is therefore needed to establish if SusP is competitive in this regime. Our second observation, negative, is that reconstruction by SusP degrades in a strong external field. Qualitatively speaking, a strong external bias overwhelms the correlations since spins do not fluctuate much, and a finite amount of data on correlated fluctuations contains less useful actionable information for the SusP reconstruction. Since the high-field limit is relevant to neural data, this may limit the applicability of SusP in this domain. In tests on one series of synthetic neural data, we indeed found that SusP does not work better than simpler schemes such as TAP.

SusP has already been extended and used for non-binary systems by Weigt et al [19]. These authors extended the SusP algorithm to Potts-like variable and successfully inferred direct physical interactions between amino acids in a family of two-component signal transduction pathways in bacteria. SusP has therefore proven its usefulness on a problem of significant biological interest. The convergence properties of this extended SusP in a suitable class of random models have however not been systematically investigated.

A The Susceptibility Propagation Algorithm

This appendix contains the update rules for the Susceptibility Propagation algorithm and their demonstration. The rules are stated in Subsection A.1, and are derived in Subsection A.2. The relation to Boltzmann machines is described in Subsection A.3.

A.1 Susceptibility Propagation Equations

Initialization: The messages $h_{i \rightarrow j}$ and $v_{i \rightarrow j, k}$ are chosen at random while the other messages $u_{j \rightarrow i}$ and $g_{i \rightarrow j, k}$ are set to 0. The couplings J_{ij} are initially also set to 0.

Update rules:

$$h_{i \rightarrow j} \leftarrow \operatorname{arctanh} m_i - u_{j \rightarrow i} \quad (5a)$$

$$g_{i \rightarrow j, k} \leftarrow \sum_{l \in \partial i \setminus j} v_{l \rightarrow i, k} + \delta_{i, k} \quad (5b)$$

$$C_{ij} \leftarrow \frac{\chi_{ij} - g_{i \rightarrow j, j}(1 - m_i^2)}{g_{j \rightarrow i, j}} + m_i m_j \quad (5c)$$

$$\tanh J_{ij} \leftarrow \epsilon \frac{C_{ij} - \tanh h_{i \rightarrow j} \tanh h_{j \rightarrow i}}{1 - C_{ij} \tanh h_{i \rightarrow j} \tanh h_{j \rightarrow i}} + (1 - \epsilon) \tanh J_{ij} \quad (5d)$$

$$\tanh u_{i \rightarrow j} \leftarrow \tanh J_{ij} \tanh h_{i \rightarrow j} \quad (5e)$$

$$v_{i \rightarrow j, k} \leftarrow g_{i \rightarrow j, k} \tanh J_{ij} \frac{1 - \tanh^2 h_{i \rightarrow j}}{1 - \tanh^2 u_{i \rightarrow j}} \quad (5f)$$

Output rules:

The couplings J_{ij} are derived in the update step. The external fields are computed from the converged messages and the magnetizations as

$$h_i \leftarrow \operatorname{arctanh} m_i - \sum_{j \in \partial i} u_{j \rightarrow i} \quad (6)$$

A.2 Deriving the SusP update rules

As a starting point, we will use the canonical update equations of Belief Propagation applied to the pairwise Ising model:

$$p_{i \rightarrow j}(\sigma_i) \propto e^{-h_i \sigma_i} \prod_{f_k \in \partial i \setminus f_j} q_{k \rightarrow i}(\sigma_i)$$

$$q_{j \rightarrow i}(\sigma_i) \propto \sum_{\sigma_j = \pm 1} e^{J_{ij} \sigma_i \sigma_j} p_{j \rightarrow i}(\sigma_j)$$

In these two equations, $p_{i \rightarrow j}$ and $q_{j \rightarrow i}$ are the messages exchanged over spins i and j , and ∂i are the spins in the neighbourhood of i . Proportionality means up to a normalization *e.g.* $\sum_{\sigma_i} p_{i \rightarrow j}(\sigma_i) = 1$ and $\sum_{\sigma_i} q_{j \rightarrow i}(\sigma_i) = 1$. Finally, to retrieve the marginals we have the following equation:

$$p_i(\sigma_i) \propto e^{-h_i \sigma_i} \prod_{f_k \in \partial i} q_{k \rightarrow i}(\sigma_i)$$

where proportionality again means up to a normalization.

For Ising spins it is convenient to work with the log-likelihood notation

$$h_{i \rightarrow j} = \frac{1}{2} \log \frac{p_{i \rightarrow j}(+1)}{p_{i \rightarrow j}(-1)}$$

$$u_{i \rightarrow j} = \frac{1}{2} \log \frac{q_{i \rightarrow j}(+1)}{q_{i \rightarrow j}(-1)}$$

which satisfy

$$h_{i \rightarrow j} = h_i + \sum_{k \in \partial i \setminus j} u_{k \rightarrow i}$$

and (in the other direction)

$$\tanh u_{i \rightarrow j} = \tanh J_{ji} \tanh h_{i \rightarrow j}$$

This is Eq. (5e) of the SusP update rules. SusP works also with the gradient of messages

$$g_{i \rightarrow j, k} = \frac{\partial h_{i \rightarrow j}}{\partial h_k}, \quad v_{i \rightarrow j, k} = \frac{\partial u_{i \rightarrow j}}{\partial h_k}$$

Their update rules are derived by differentiating the update rules of the messages with respect to external fields, and give

$$g_{i \rightarrow j, k} = \sum_{l \in \partial i \setminus j} v_{l \rightarrow i, k} + \delta_{i, k}$$

and

$$v_{i \rightarrow j, k} = g_{i \rightarrow j, k} \tanh J_{ij} \frac{1 - \tanh^2 h_{i \rightarrow j}}{1 - \tanh^2 u_{i \rightarrow j}}$$

These are Eqs. (5b) and (5f) of the SusP update rules.

The log-likelihood quantities describing the marginals are the effective fields $H_i = \frac{1}{2} \log \frac{p_i(+1)}{p_i(-1)}$. *Exact* effective fields are related to magnetizations m_i and correlation functions χ_{ij} by

$$m_i = \tanh H_i$$

and (by fluctuation-dissipation)

$$\chi_{ij} = \frac{\partial \tanh H_i}{\partial h_j}$$

On the other hand, in Belief Propagation the effective fields are related to the log-likelihood messages as

$$H_i = h_i + \sum_{j \in \partial i} u_{j \rightarrow i}$$

Combining the two, or, what is the same, taking the Belief Propagation computed effective fields as proxies for the exact effective fields, we have

$$h_i = \tanh^{-1}(m_i) - \sum_{j \in \partial i} u_{j \rightarrow i}$$

which is Eq. (6), the SusP output rule. Substituting h_i from above into the update equation for $h_{i \rightarrow j}$ we have

$$h_{i \rightarrow j} = \tanh^{-1}(m_i) - u_{j \rightarrow i}$$

which is Eq. (5a) of the SusP update rules.

If the correlation functions χ_{ij} are expressed in terms of the partial derivatives of the effective fields, and the effective fields are computed by Belief Propagation, then we will show that

$$\chi_{ij} = \overline{\chi_{ij}} g_{j \rightarrow i, j} + g_{i \rightarrow j, j} (1 - m_i^2) \quad (7)$$

where the auxiliary quantities $\overline{\chi_{ij}}$ are

$$\overline{\chi_{ij}} = \frac{\tanh J_{ji} + \tanh h_{i \rightarrow j} \tanh h_{j \rightarrow i}}{1 + \tanh J_{ji} \tanh h_{i \rightarrow j} \tanh h_{j \rightarrow i}} - m_i m_j \quad (8)$$

These equations do not (in general) hold exactly, but only under the assumption that Belief Propagation is exact. If and when so, then by fluctuation-dissipation

$$\begin{aligned} \chi_{ij} &= \frac{\partial \tanh H_i}{\partial h_j} = \frac{\partial m_i}{\partial h_j} \\ &= \frac{\partial (h_i + \sum_{j \in \partial i} u_{j \rightarrow i})}{\partial h_j} (1 - m_i^2) \\ &= \frac{\partial (h_{i \rightarrow j} + u_{j \rightarrow i})}{\partial h_j} (1 - m_i^2) \\ &= (v_{j \rightarrow i, j} + g_{i \rightarrow j, j}) (1 - m_i^2) \end{aligned}$$

To show Eq. (7) and Eq. (8) we hence have to prove that $v_{j \rightarrow i, j} (1 - m_i^2) = \overline{\chi_{ij}} g_{j \rightarrow i, j}$, which is the same as

$$\frac{1 - c^2}{1 - a^2 c^2} \left(1 - \left(\frac{b + ac}{1 + abc} \right)^2 \right) = \frac{a + bc}{1 + abc} - \frac{c + ab}{1 + abc} \times \frac{b + ac}{1 + abc} \quad (9)$$

using the shorthand

$$a = \tanh J_{ij} \quad b = \tanh h_{i \rightarrow j} \quad c = \tanh h_{j \rightarrow i}$$

such that

$$m_i = \frac{b + ac}{1 + abc} \quad m_j = \frac{c + ab}{1 + abc} \quad \tanh u_{j \rightarrow i} = ac$$

Eq. (9) is an algebraic identity, as can be verified by termwise comparison, which therefore shows Eq. (7) and Eq. (8).

In the final step we express J_{ij} as a function of χ_{ij} and all the other quantities. It is convenient to first introduce yet another auxiliary quantity

$$C_{ij} = \frac{\chi_{ij} - g_{i \rightarrow j, j} (1 - m_i^2)}{g_{j \rightarrow i, j}} + m_i m_j \quad (10)$$

which is Eq. (5c) of the SusP update rules. In Eq. (10) the correlations χ are from data. If, on the other hand, we substitute Eq. (7) and Eq. (8) into Eq. (10) we have

$$C_{ij} = \frac{\tanh J_{ji} + \tanh h_{i \rightarrow j} \tanh h_{j \rightarrow i}}{1 + \tanh J_{ji} \tanh h_{i \rightarrow j} \tanh h_{j \rightarrow i}} \quad (11)$$

which can be inverted to

$$\tanh J_{ji} = \frac{C_{ij} - \tanh h_{i \rightarrow j} \tanh h_{j \rightarrow i}}{1 - C_{ij} \tanh h_{i \rightarrow j} \tanh h_{j \rightarrow i}} \quad (12)$$

which is Eq. (5d), the final update rule for SusP, and also the central step (Eq. (1)) quoted in the bulk of the paper.

A.3 Relation of SusP to Boltzmann machines

We recall that the Boltzmann machine approach consists of the iterative procedure

$$\delta J_{ij} = \eta (\chi_{ij}^{\text{Data}} - \chi_{ij}^{\text{Model}}) \quad (13)$$

In practical applications this is often prohibitively expensive, because the correlations χ_{ij}^{Model} have to be evaluated by Monte Carlo. Eq. (7) and Eq. (8) are a means to quickly (if approximately) evaluate the correlations χ_{ij}^{Model} using Belief Propagation variables and gradients of Belief Propagation variables.

The fixed point of a Boltzmann machine approach must satisfy the set of equations

$$\chi_{ij}^{\text{Data}} = \chi_{ij}^{\text{Model}}(\{J_{ij}\}) \quad (14)$$

where we have made explicit that the correlations χ_{ij}^{Model} depend on all the model parameters $\{J_{ij}\}$. Eq. (7) is of just this form, and so is Eq. (11) for the auxiliary quantities C_{ij} . A standard way to solve such equations would be by the Newton method or other general-purpose root-finding methods. Eq. (12) however means to solve each equation for χ_{ij} separately by varying the corresponding J_{ij} , and keeping all else fixed.

Iterating Belief Propagation until convergence and then inverting locally for J_{ij} potentially wastes computation

time in iterations. The actual scheme of [7] described above is therefore to interleave Belief Propagation update steps (including updating the BP gradient quantities), and locally solving for J_{ij} . This explains the order of the operations stated in A.1. Convergence of this scheme is however not an easy question to answer. Presumably there can be complications analogous to using Newton method in a high-dimensional situation (one has to have a good starting point), but as discussed in the bulk of the paper, there also seem to be other effects (eigenvalue cross-over before the spin glass transition).

References

1. D. H. Ackley, G. E. Hinton, and T. J. Sejnowski. A learning algorithm for boltzmann machines. *Cognitive Science*, 9:147–169, 1985.
2. S. Cocco, S. Leibler, and R. Monasson. Neuronal couplings between retinal ganglion cells inferred by efficient inverse statistical physics methods. *Proc Natl Acad Sci U S A*, 106:14058–62, 2009.
3. H. J. Kappen and F. B. Rodriguez. Efficient learning in boltzmann machines using linear response theory. *Neur. Comp.*, 10:1137–1156, 1998.
4. T. R. Lezon, J. R. Banavar, M. Cieplak, A. Maritan, and N. Fedoroff. Using the principle of entropy maximization to infer genetic interaction networks from gene expression patterns. *Proc. Natl. Acad. Sci.*, 103, 2006.
5. E. Marinari and V. V. Kerrebroeck. Intrinsic limitations of the susceptibility propagation inverse inference for the mean field ising spin glass. *J. Stat. Mech.*, 2010.
6. M. Mézard and A. Montanari. *Information, Physics and Computation*. Oxford University Press, 2009.
7. M. Mézard and T. Mora. Constraint satisfaction problems and neural networks: A statistical physics perspective. *Journal of Physiology-Paris*, 103:107–113, 2009.
8. J. M. Mooij and H. J. Kappen. Loop corrections for approximate inference on factor graphs. *Journal of Machine Learning Research*, 8:1113–1143, 2007.
9. C. Ollion. Susceptibility Propagation for the inverse Ising Problem, 2010.
10. P. Ravikumar, M. Wainwright, and J. D. Lafferty. High-dimensional ising model selection using l_1 -regularised logistic regression. *Annals of Statistics*, 2010. (to appear).
11. Y. Roudi, J. A. Hertz, and E. Aurell. Statistical physics of pairwise probability models. *Front. Comput. Neurosci.*, 3, 2009.
12. Y. Roudi, S. Nirenberg, and L. P. E. Pairwise maximum entropy models for studying large biological systems: when they can work and when they can't. *PLoS Comp. Biol.*, 5:e1000380, 2009.
13. Y. Roudi, J. Tyrcha, and J. Hertz. Ising model for neural data: Model quality and approximate methods for extracting functional connectivity. *Phys. Rev. E*, 79(5):051915, May 2009.
14. E. Schneidman, M. Berry, R. Segev, and W. Bialek. Weak pairwise correlations imply strongly correlated network states in a neural population. *Nature*, 440:1007–1012, 2006.
15. V. Sessak and R. Monasson. Small-correlation expansions for the inverse ising problem. *J. Phys. A: Math. Theor.*, 42, 2009.
16. D. Sherrington and S. Kirkpatrick. Solvable model of a spin-glass. *Phys. Rev. Lett.*, 35:1792 – 1796, 1975.
17. J. Shlens, G. Field, J. Gauthier, M. Grivich, D. Petrusca, A. Sher, A. Litke, and E. Chichilnisky. The structure of multi-neuron firing patterns in primate retina. *J. Neurosci.*, 26:8254–8266, 2006.
18. T. Tanaka. Mean-field theory of boltzmann machine learning. *Phys. Rev. E*, 58:2302–2310, 1998.
19. M. Weigt, R. A. White, H. Szurmant, J. A. Hoch, and T. Hwa. Identification of direct residue contacts in protein-protein interaction by message passing. *PNAS*, 106:67–72, 2009.
20. J. S. Yedidia, W. T. Freeman, and Y. Weiss. *Understanding Belief Propagation and its Generalizations*, pages 239–269. Science & Technology Books, 2003.